



**HAL**  
open science

## Fractal scattering indicators for urban sound diffusion

Philippe Woloszyn

► **To cite this version:**

Philippe Woloszyn. Fractal scattering indicators for urban sound diffusion. Miroslav M. Novak. Thinking in Patterns. Fractals and Related Phenomena in Nature, World Scientific, pp.221, 2004, 981-238-822-2. 10.1142/9789812702746\_0018 . hal-01552973

**HAL Id: hal-01552973**

**<https://hal.science/hal-01552973v1>**

Submitted on 3 Jul 2017

**HAL** is a multi-disciplinary open access archive for the deposit and dissemination of scientific research documents, whether they are published or not. The documents may come from teaching and research institutions in France or abroad, or from public or private research centers.

L'archive ouverte pluridisciplinaire **HAL**, est destinée au dépôt et à la diffusion de documents scientifiques de niveau recherche, publiés ou non, émanant des établissements d'enseignement et de recherche français ou étrangers, des laboratoires publics ou privés.

See discussions, stats, and author profiles for this publication at: <https://www.researchgate.net/publication/269192987>

# Fractal scattering indicators for urban sound diffusion

Chapter · January 2004

DOI: 10.1142/9789812702746\_0018

---

CITATION

1

READS

27

1 author:



[Philippe Woloszyn](#)

French National Centre for Scientific Research

99 PUBLICATIONS 209 CITATIONS

[SEE PROFILE](#)

Some of the authors of this publication are also working on these related projects:



HAUP HyperAmbiotopes Urbains Participatifs [View project](#)

All content following this page was uploaded by [Philippe Woloszyn](#) on 30 April 2015.

The user has requested enhancement of the downloaded file. All in-text references [underlined in blue](#) are added to the original document and are linked to publications on ResearchGate, letting you access and read them immediately.

# FRactal Scattering Indicators for Urban Sound Diffusion

PHILIPPE WOLOSZYN

*Cerma UMR CNRS 1563, Ecole d'Architecture de Nantes, BP 81931*

*F-44319 Nantes Cedex 3, France*

*E-mail : [philippe.woloszyn@cerma.archi.fr](mailto:philippe.woloszyn@cerma.archi.fr)*

Irregular surfaces like urban frontages produce an anomalous back-scattered region, creating an acoustic interference field in their neighborhood. Thus, in order to be able to detect that scattered energy's minima and maxima through taking the frontage morphological characterization into account, we propose a new measurement method of the building geometry, with using mathematical morphology techniques. Results of this geometrical approach provide two types of indicators, global and local. The global one, the structure factor of the urban frontage, is related to the multiscale characterization of the whole building geometry through the computation of the spatial Fourier transform of the scatterers. The complementary local indicator evaluates the vertex multiscale densitometrical distribution at each incidence angle, provided through a fractal evaluation technique, the Minkowski sausage. This densitometry computation reveals the characteristic directions of scattering, which has to be calculated through the scattering pressure function along the lateral active diffraction zone.

Keywords: Acoustic Diffusion, Scattering, Minkowski Sausage.

## 1 Introduction: Problematic and purpose

The exterior frontage of a typical urban building does not reflect noise in a purely specular manner. Because the dimensions of the irregularities (decorative elements, windows, balconies,...) are comparable to the sound wavelengths, the major type of early reflexions on the buildings is scattering, inducing a global diffusion behaviour of sound in an urban street. Consequently, irregular surfaces like urban frontages produces an anomalous back-scattered region, with the creation of an acoustic interference field in its neighborhood. Thus, in order to be able to detect that scattered energy's minima and maxima, we have to take into account both incidence angle and multiscale characterization for diffusive evaluation of urban surfaces through mathematical morphology techniques.

## 2 Diffusion through oblique incident wave

### 2.1 A first approximation: the Rayleigh criterion

Historically, the first attempt at determining the scattering amplitudes was made in 1893 by Lord Rayleigh, who assumed a unique solution for the wave equation for the whole boundary of a  $\Lambda$ -corrugated surface [1]. Concerning the inferior diffusion limit frequency, Rayleigh's work proposes a phase grating calculation between two acoustic rays related in [2], which takes into account the source incidence angle. Taking the walk difference  $\Delta d$  between two rays with wavelength  $\lambda$  and incidence angle  $\alpha$  regarding a surface with depth  $\Lambda$  into account provides the following phase grating calculation between the two rays:

$$\Delta\alpha = \Delta d (2\pi / \lambda) = \cos \alpha (4 \pi \Lambda / \lambda) \quad (1)$$

with the walk difference :  $\Delta d = 2 \Lambda \cos \alpha$ . For a weak walk difference  $\Delta d$ , rays are coherent and the acoustic wave is specularly reflected. Increasing of  $\Delta d$  will interfere rays, till to phase opposition ( $\Delta d = \pi$ ), so that no energy is displayed in the specular direction : sound energy is diffused. Rayleigh criterion defines the limit between specular and diffuse behaviour of an incident source, corresponding to the frontage depth irregularities as :  $\Lambda < 1 / 8 \cos \alpha$ .

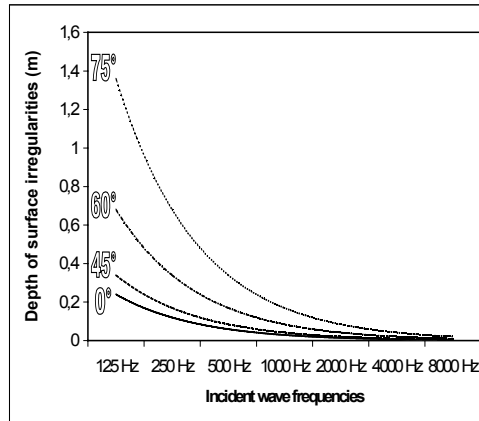


Fig. 1. Rayleigh criterion: Quantification of the dimensional limit between specularity and diffusion, as a function of frequency and incidence angle.

The specular reflexion zone is defined under the minimal values of the frontages depths irregularities, taking the frequency and the angle of the incident wave into account.

## 2.2 Diffraction densitometry of an indented plane

Following those non-specularity conditions, the propagation directions specified by the unit vectors  $\mathbf{v}(d) = (\phi_d, \theta, \gamma_d)$  for a given regular plane division, repeating  $n$  times a spatial unit of width  $\Lambda$  are defined as the *characteristic directions of scattering* associated with the localization length  $\Lambda$ :

$$\sin \alpha_d = \frac{p\lambda}{2n\Lambda} - \sin \alpha, \quad (2)$$

where  $\alpha_d$  is the grazing diffraction angle made by vectors  $\mathbf{v}(d) = (\phi_d, \theta, \gamma_d)$  in the direction  $\theta x$ , with  $\phi_d = \cos \alpha_d$  and  $\gamma_d = \sin \alpha_d$ , and  $p$  the diffraction order. For  $\Lambda = 0$ , equality between incident and reflected angle remaining true (specular conditions).

We can note here that, ignoring the specular component  $\sin \alpha$ , the first term of the previous equation can be compared to Bragg's Law, leading to the following expression:

$$\sin \alpha = \frac{p\lambda}{2d}, \quad (3)$$

where the integer  $p$  is the order of diffraction,  $d = n\Lambda$ , the distance between two reflexion planes,  $\lambda$ , the wavelength of the incident beam and  $\alpha$  its incidence angle.

This law, also used in the field of cristallographic diffractometry, enounces the conditions for constructive interference rays, which are producing strong diffraction. Through this equation, Sir W.H. Bragg and his son developed a simple semi-quantitative model to express the diffraction from 3-D crystals, explaining why the cleavage faces of crystals

appear to reflect X-rays beams at certain angles of incidence. Considering those crystal structures as families of parallel planes ( $hx, ky, lz$ ) running in different directions, each plane acts like a slightly reflective mirror, reflecting a tiny fraction of the incident beam. When in phase, those reflections lead to constructive interference rays, conditioned with Bragg's Law's equation. For  $p=1$ , all planes inside the cosine scatter in phase, providing maximal diffraction. For  $p=1-\Lambda$ , the diffraction cancels.

In the same way, Bragg's law and Rayleigh criterion defines the conditions of interfering behaviour, for acoustic waves reflected on micrometer or meter-scaled parallel planes.

Consequently, the pure diffracted energy part of an urban indented surface can be expressed through Bragg's Law, considering the path difference between two frontage surfaces, as between two crystal planes for the constructive interference conditions:  $p\lambda=2n\Lambda \sin\alpha$ , where  $n\Lambda$  is the frontage indentation depth.

Moreover, the two-dimensional polar response of a given indented surface can be expressed through the diffraction orders ( $p, q$ ), taking the angles of incidence and diffraction into account:

$$\sqrt{p^2 + q^2} = n\Lambda \frac{\sin \alpha_d + \sin \alpha}{\lambda} \quad (4)$$

The characteristic directions are those along which the waves emanating from the individual frontage indentation depth  $\Lambda$  are exactly in phase. This constructive interference condition is both conditioned with the adimensional modulus  $\Lambda / \lambda$ , which quantifies the energy of non-evanescent scattering losses, represented by the area of scattering intensity pattern lobes, and with the previous Bragg's equation  $p\lambda=2n\Lambda \sin\alpha$ . Indeed, this modulus is conditioning the solutions of equation (4), as  $\Lambda / \lambda = 0$  traduces specular reflection (as the diffraction order  $p$  is null through the limit of the diffusion), and as this modulus value conditions its number of real solutions, corresponding to the diffraction directions (lobes of the surface's radiated energy).

### 3 Diffraction and structure factor of a multiscale rough boundary surface

For all other directions, the reflected waves will destructively interfere, resulting in complete cancellation for a self-similar periodic structure. For non- or pre-fractal structures as urban frontages, the scattered field will show mainlobes in the characteristic directions, and sidelobes elsewhere for a done sound frequency).

#### 3.1 Phase of diffraction

Those interference conditions can be also expressed with defining the phases of the incident wave vector  $\mathbf{k}_0$  and the diffracted vector  $\mathbf{k}$ , which both have an amplitude equal to the reciprocal of the wavelength. In order to calculate the phase of the diffracted wave, taking the path lengths difference  $\Delta d = 2 n\Lambda \cos\alpha$  into account, we will consider the difference between the path of the sonic particle (phonon) along the incident beam  $\mathbf{k}_0\mathbf{r}$  and its path along the diffracted beam  $\mathbf{k}\mathbf{r}$ . With expressing this path length difference  $\Delta d = 2 n\Lambda \cos\alpha = \mathbf{k}_0\mathbf{r} - \mathbf{k}\mathbf{r}$ , the overall diffraction phase will be expressed as  $-2\pi(\mathbf{k}_0\mathbf{r} - \mathbf{k}\mathbf{r}) = 2\pi(\mathbf{k} - \mathbf{k}_0)\mathbf{r}$  (figure 2).

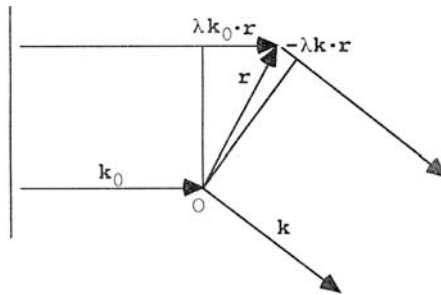


Fig. 2. Phase geometry

Considering  $|\mathbf{r}| \cos \alpha$ , the component of  $\mathbf{r}$  in the direction of the diffraction vector  $\mathbf{s}$ , all points with the same value of  $\mathbf{s}\mathbf{r}$  are lying on a plane perpendicular to vector  $\mathbf{s}$ , allowing the same diffraction phase (figure 3).

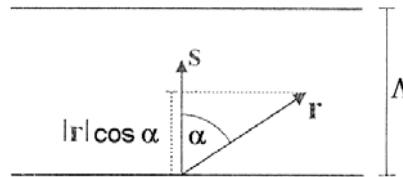


Fig. 3. Diffraction geometry

Consequently, as the length of the diffraction vector  $|\mathbf{s}|$  is equal to  $1/\Lambda$  (inverse of the indentation depth),  $\mathbf{s}\mathbf{r}$  is equal to the distance between two Bragg planes (or indentation surfaces), and diffraction from any point  $r$  will have a phase of  $2\pi\mathbf{s}\mathbf{r}$ .

Moreover, we can define the phonon density resolution through the mean resolution distance, according to the period  $n\Lambda$  of the Fourier serie of the phonon density map. The following equation leads us to the calculus of the reflective resolution of the structure, involving the path difference  $\Delta d$  as:

$$\frac{1}{\Delta d} = \sqrt{\frac{h^2}{a^2} + \frac{k^2}{b^2} + \frac{l^2}{c^2}} = \frac{1}{2\Lambda \cos \alpha} \quad (5)$$

where  $(h, k, l)$ , the Miller indices, specify the direction and the period of the tridimensional cosine wave  $\cos(2\pi/[hx/a + ky/b + lz/c])$ .

### 3.2 Structure factor indications: spatial scattering function

When measuring several phonons located at different points, the diffraction at each point will be the sum of the waves scattered by each phonon. So, the expression of this sum with Euler's equation gives us, for the  $j^{\text{th}}$  phonon with coordinates  $(x_j, y_j, z_j)$ :

$$F(\mathbf{s}) = \sum_j \exp(2\pi i \mathbf{s} \cdot \mathbf{r}_j) \quad (6)$$

This wave is represented here by its *structure factor*, which is the Fourier transform of the scatterers of equal strength on all points of the diffraction plane. Continuous expression of this previous equation involves the phonon's density  $\rho(\mathbf{r})$  as:

$$F(\mathbf{s}) = \int_{\text{space}} \rho(\mathbf{r}) \exp(2\pi i \mathbf{s} \cdot \mathbf{r}) d\mathbf{r} \quad (7)$$

As shown through this expression of the structure factor, the diffraction pattern is defined as the Fourier transform of the phonon density.

Taking into account the tridimensional distribution of phonons into the diffusive structure involving Miller indices  $(h, k, l)$ , as the plane perpendicular to vector  $s$  can be written as:  $\mathbf{sr}_j = hx_j + ky_j + lz_j$ , we can afford the previous spatial expression of the structure factor in the three dimensions of space with integrating the tridimensional cosine wave as:

$$F_{hkl} = \iiint_{\text{PhononVolume}} \rho(x, y, z) \exp(2\pi i(hx + ky + lz)) dx dy dz \quad (8)$$

The acoustic field is then expressed through the phonon's density  $\rho(x, y, z)$ , which is useful to calculation of the mean square diffracted sound pressure  $P_d$  by the whole volume for a given distance of the structure [3]:

$$P_d^2 = \rho \iiint_V \frac{\cos \alpha \cos \alpha_d}{\pi r_0^2} P^2 dV \quad (9)$$

where  $r_0$  represents the distance from the receiver to the structure, and  $P$  the incident wave pressure. One can remark that the function of the cosine of the angle between the direction of observation and the normal to the surface in the observation point reminds us the Lamberts law [4], which is assumed to represent the physical behaviour of sound or light after reflection on an ideally diffusing surface. As mentioned previously, the angular repartition of the sound energy is computed with the Miller indices, involved through the individual phase contributions  $2\pi i(hx_j + ky_j + lz_j)$ , which represents the *spatial scattering function* of the reference volume  $V$  (equation (8)).

### 3.3 Dynamic scattering function

This leads us to consider the structure factor as a function of time, called *dynamic structure factor*, or *dynamic scattering function*, with introducing time  $t$  through a random walk in random environment [5]:

$$F(\mathbf{s}, \omega) = 2 \int_0^\infty \cos(\omega, t) \rho(\mathbf{r}, t) dt \quad (10)$$

The dynamical density distribution  $\rho(\mathbf{r}, t)$  can be obtained with the probability for a sonic particle to walk to location  $\mathbf{r}$  during the time  $t$   $P(\mathbf{r}, t)$ , that remains equation (5), with the following relationship [6]:

$$\rho(\mathbf{s}, i\omega) = \int d\mathbf{r} \exp(i\mathbf{s}\mathbf{r}) \int_0^\infty dt \exp(-i\omega t) P(\mathbf{r}, t) \quad (11)$$

with  $P(\mathbf{r}, t)$ , describing the sonic particle's probability for a *fractional Brownian walk* in a non-integer (fractal)  $D$ -dimensional space [7], [8]:

$$P(\mathbf{r}, t) \rightarrow \frac{1}{(4\pi\delta t)^{D/2}} \exp\left(-\frac{r^2}{4\delta t}\right), N \rightarrow \infty \quad (12)$$

where  $\delta$  is the diffusion coefficient of the  $D$ -dimensional structure.

### 3.4 Angular distribution function

This function can be evaluated using a Laplace transform [9]. After integrating over the angles, we obtain, for the  $p_d^{\text{th}}$  diffraction order:

$$\rho(\mathbf{s}, i\omega) = \frac{2\pi g}{i\omega^{1-D/d_w}} \int dr \mathbf{r}^{D-1} \frac{\sin(p_d \mathbf{r})}{p_d \mathbf{r}} * \frac{1}{(i\omega \mathbf{r}^{1/d_w})^{D-1/2}} \exp(-i\omega \mathbf{r}^{1/d_w} / g) \quad (13)$$

where  $D$  is the fractal dimension of the diffusive structure,  $d_w$  the parametering of the random walk of the phonon [10], and  $g$  is the *angular distribution function* along a characteristic direction of scattering:

$$g(\mathbf{r}) = \frac{1}{m^2} (G_0(\mathbf{r}) - \bar{m} \rho(\mathbf{r})) \quad (14)$$

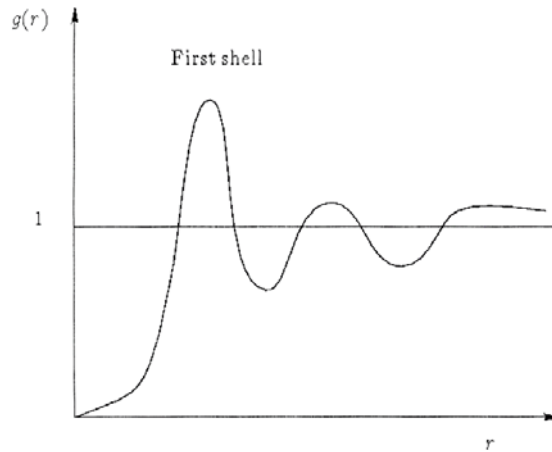


Fig. 4. Typical angular distribution function. The first shell represents the main density function at a distance  $r$  of the structure.

$G_0 = \langle m(o)m(\mathbf{r}) \rangle$  is the second moment of density taken in the points  $o$  and  $r$ , called *density-density correlation function*. Square of the average density  $\bar{m} = \sum_i \rho(\mathbf{r}_i)$

constitutes the limit of the density-density correlation function  $G_0$  when  $\mathbf{r} \rightarrow \infty$ :

$G_0(\mathbf{r}) \rightarrow \bar{m}^2$  and  $g(\mathbf{r}) \rightarrow 1$ . This function defines the scattering intensity of the structure for a defined angle as:

$$I_q = \int_j G_0(\mathbf{r})^{-iqr} dr \quad (15)$$

### 3.5 Parseval theorem and diffusion volume

Parseval's theorem formulates that the energy in the frequency domain is the same as the energy in the spatial domain [11]. Consequently, the mean square value on one side of the Fourier transform equation (8) is proportional to the mean square value on the other side. So do Parseval's theorem allows to express the phonons density distribution as a transform of the spatial distribution of the surface scatterers. This property allows us to express the angular distribution function as a discrete quadratic summation of elementary structure factors as following:

$$\int_V \rho(x, y, z)^2 dV = \frac{1}{V_{xyz}} \sum_{hkl} |F_{hkl}|^2, \quad (16)$$



where the diffusion volume  $V_{xyz}$  is a ratio between the square root of the discrete quadratic summation of the structure factors and the angular distribution function. This diffusion volume  $V_{xyz}$  is experimentally obtained by a mathematical morphological measure using a Minkowski operator, which provides a ribbon surface constituting a neighborhood area, under the condition of continuity [12]. Considering the Minkowski analysis of a tridimensional structure, structured with a structuring element of variable radius  $\Lambda$ , the phonons density-density distribution can be expressed through the roughness autocorrelation of the diffusive structure with involving the *diffusion volume*  $V_{xyz}$ , and the structure factor  $F_{hkl}$ , which defines both the global and local behavior of the structure as:

$$\rho(x, y, z) = \sqrt{\frac{\sum_0^{\Lambda_{\max}} |F_{hkl}|^2}{V_{xyz}}} \propto V_{xyz} \sum_0^{\Lambda_{\max}} \sin \alpha_d + \sin \alpha \quad (17)$$

#### 4 Application : a Frontage scattering characterization

##### 4.1 The urban frontage model

The spatial configuration we measure here is a numerical 3-D model of a neoclassical frontages of an urban street of Nantes, France, the *rue d'Orléans*, belonging to a 19<sup>th</sup> urban morphology type, with windows, doors, and freestone casting off. One of the main characteristics of this type of architecture is the relative exuberance of its frontage structure, following neo-classical composition. This frontage is considered as a tridimensional object situated in an ortho-normed space, rotating around the Z-axis (Fig. 5):

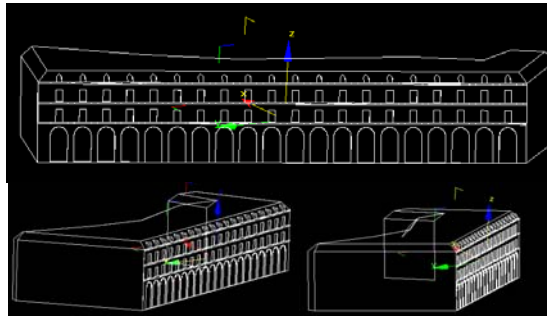


Fig. 5. Orthographical rotative analyze of a frontage in the *rue d'Orléans*, Nantes.

##### 4.2 The Minkowski measurement technique

In order to characterize the scattering behavior of the volume of the frontage, we apply a fractal Minkowski operator, called Minkowski sausage, to evaluate the vertex multiscale densitometry distribution at each incidence angle. This operator consists into replacing each point of the vertexes of the urban geometry with a sphere with variable radius  $\Lambda$ , as seen figure 6:

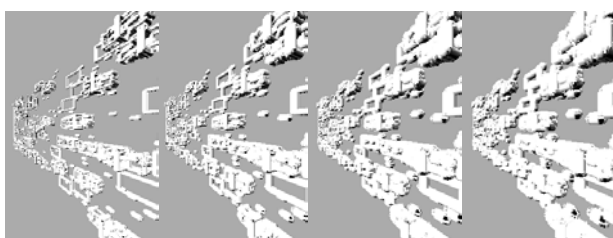


Fig. 6. Tridimensional dilation of the urban scene vertexes (perspective views).

This transformation of the urban geometry corresponds to the *dilation* operation in the morpho-mathematical context [12]. The union of all spheres is called the *3-D Minkowski sausage*. The variation of their diameter gives us successive approached perimeter/surface ratios at each vision angle, which regression evaluates the fractal dimension of the structure, in a specified validity domain.

#### 4.3 Frontage fractal measurement

The spatial multiscale evolution of the perimeter-surface ratio  $P/S$  defines the profile's *Shape spectrum* of the frontage [13]. This spectrum defines the multiscale relationship between the radius evolution of the spherical structuring element and the "mass" of the structure, for each the angular measure. As readable in the following figure, the specular domain is illustrated with a strong decrease of the  $P/S$  ratio, which corresponds to the limit  $A_{max}$  for the radius of the structuring element. For this domain, the Euclidean dimension  $d$  and the fractal dimension  $D$  of the mean structure reach the same value. This break in the frontage indentations shape spectrum behavior occurs for  $A_{max}=100$  cm, for every value of incidence angle  $\alpha$  (figure 7):

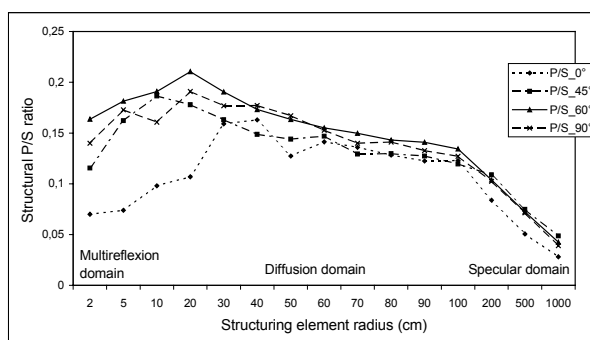


Fig. 7. Shape spectrums of the urban frontage with a spherical recovering element, at different incident angles.

#### 4.4 Results of the analysis : Frontage's structure factors and vertex densitometry

The Fourier transform of the surface roughness informs the frontage's complexity, leading both to the angular distribution function and the spatial scattering function of the indented surface calculations.

As an indicator of the indentations frequency, the Fourier transform discriminates clearly the structure of a surface, revealing the spatial occurrences of the roughness peaks (figure 8.1).

The angular distribution function is defined through the structure factor computation of the surface, and indicates the frontage scattering behaviour for a particular direction of the incident beam (figure 8.2).

Moreover, the spatial scattering function offers a tridimensional interpretation of the angular distribution function, allowing the distribution of the surface's scatterers along every incidence angle of the acoustic source (figure 8.3).

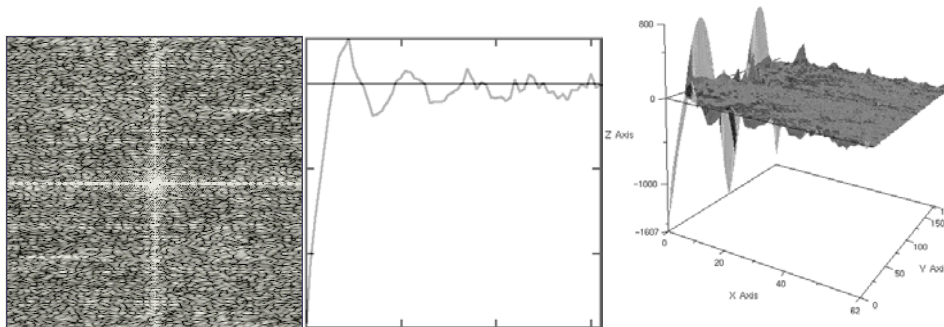


Fig. 8. Fourier transform (1), angular distribution function (2) and spatial scattering function (3) of the frontage indented surface

Those indicators allows the computation of the vertex densitometry for every incidence angle of the surface, with an increment of 5 degrees for localisation lengths  $\lambda$  from 0.05 to 10 m, which corresponding acoutical frequency domain is 25 Hz to 8 kHz. Those densitometries correspond to the characteristic directions of scattering, through the density distribution  $\rho(x, y, z)$  calculation for each incidence angle.

This angular evaluation of the vertexes distribution shows azimuthal densitometries due to interreflexions of the corners and the freestone casting along three windows depth, corresponding to the lateral active diffraction zone.

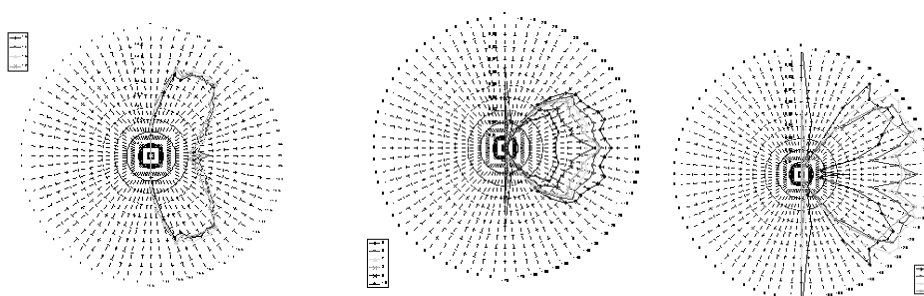


Fig. 9. Angular vertex densitometry of the urban frontage applied to the urban scene. Measures for roughness values  $r$  of, respectively, 1 to 10 m, 0.2 to 0.5 m and 0.05 to 0.2 m .

Global polar responses for growing localisation lengths shows globally a decreasing diffusivity, revealing a bilobe distribution structure of the biggest scatterers, a cardioid for middle-sized ones and very characteristic peaks for high frequency roughness.

## 5 Conclusion

Through the determination of the structure factor, the Minkowski sausage technique provides a quantification of the scatter distribution function of the indented surface of a specified urban neo-classical frontage at each incidence angle. In order to perform an experimental validation of this model, experimental results will be compared to those indicators at each incidence angle, through an in situ and a 1/10<sup>th</sup> scale model MLS multisensor measurement.

With discerning the angular vertex densitometry of main types of architectures, we will be able to compute their specific angular spatial scattering function for every frequency, directly from the Minkowski analysis of the numerical 3-D model of their geometry. Through those morphological treatment of architectural shapes, this research work will confirm the definition of the diffusion process as a geometrical-dependant phenomenon, influenced by the built structure on urban acoustics.

## 6 References

1. Lord Rayleigh, "The theory of Sound", Vol. 2, *Dover ed*, New-york, 1945, pp. 89-96.
2. Beckmann P., Spizzichino A., 1987 "The Scattering of Electromagnetic Waves from Rough Surfaces", *Artec House, INC*, Norwood.
3. R. Makarewicz & P. Kokowski, "Reflexion of noise from a building's facade", *Applied Acoustics* **43**, London, 1994, pp.149-157.
4. Lewers T, "A Combined Beam Tracing and Radiant Exchange Computer Model of Room Acoustics", *Applied Acoustics* **38** (1993), pp. 161-178.
5. Hollander and al., "Dynamic Structure Factor in a Random Diffusion Model", *Journal of Statistical Physics*, Vol.76, **5:6**, 1994.
6. Roman, 1997, "Diffusion on self-similar structures", *Fractals, World Scientific*, Vol. 5, **3**, September 1997 pp.379-393.
7. Gouyet J.F. : "Physique et structures fractales", Paris, *Masson ed*, 1992, 234 p.
8. Mandelbrot, B., « Les objets fractals », Paris, *Flammarion ed*, 1992.
9. Roman H.E. : *Phys. Rev.* **E51**, 5422 (1995).
10. Woloszyn P. : "Mesures multiéchelles du tissu urbain et paramétrage d'un modèle de diffusion acoustique en milieu construit", *ed. ENPC*, Marne-la-Vallée, 1997.
11. Young P., "Parceval's Theorem", *Physics* **114 A**, 1999.
12. Pfeiffer P., Obert M. & Cole M.W. : "Fractal BET and FHH theories of adsorption: a comparative study", *Proc. R. Soc. Lond.* **A423**, pp. 169-188, 1989.
13. Woloszyn P. : "Squaring the circle : diffusion volume and acoustic behavior of a fractal structure", *ed. M. M. Novak, World Scientific Publishing*, Singapour, 2000, pp. 299-300.